

Featuring work from the Warkiani lab at the School of Mechanical and Manufacturing Engineering and Australian Center for Nanomedicine at the University of New South Wales, Sydney, Australia. (Artwork by Mehdi Rafeie from the School of Mechanical and Manufacturing Engineering, University of New South Wales).

Title: Flow-induced stress on adherent cells in microfluidic devices

Transduction of mechanical forces and chemical signals affects every cell in the human body. This review discusses recent advances in microfluidic systems for studying flow-induced effects on adherent cells and elaborates on their suitability to mimic physiologic microenvironments, with important applications in the cardiovascular, stem cell and cancer biology fields.

As featured in:



See Majid Ebrahimi Warkiani et al.
Lab Chip, 2015, 15, 4114.

Cite this: *Lab Chip*, 2015, 15, 4114

Flow-induced stress on adherent cells in microfluidic devices

Jonathan Shemesh,^a Iman Jalilian,^b Anthony Shi,^a Guan Heng Yeoh,^a Melissa L. Knothe Tate^b and Majid Ebrahimi Warkiani^{*ac}

Transduction of mechanical forces and chemical signals affect every cell in the human body. Fluid flow in systems such as the lymphatic or circulatory systems modulates not only cell morphology, but also gene expression patterns, extracellular matrix protein secretion and cell-cell and cell-matrix adhesions. Similar to the role of mechanical forces in adaptation of tissues, shear fluid flow orchestrates collective behaviours of adherent cells found at the interface between tissues and their fluidic environments. These behaviours range from alignment of endothelial cells in the direction of flow to stem cell lineage commitment. Therefore, it is important to characterize quantitatively fluid interface-dependent cell activity. Common macro-scale techniques, such as the parallel plate flow chamber and vertical-step flow methods that apply fluid-induced stress on adherent cells, offer standardization, repeatability and ease of operation. However, in order to achieve improved control over a cell's microenvironment, additional microscale-based techniques are needed. The use of microfluidics for this has been recognized, but its true potential has emerged only recently with the advent of hybrid systems, offering increased throughput, multicellular interactions, substrate functionalization on 3D geometries, and simultaneous control over chemical and mechanical stimulation. In this review, we discuss recent advances in microfluidic flow systems for adherent cells and elaborate on their suitability to mimic physiologic micromechanical environments subjected to fluid flow. We describe device design considerations in light of ongoing discoveries in mechanobiology and point to future trends of this promising technology.

Received 9th June 2015,
Accepted 22nd August 2015

DOI: 10.1039/c5lc00633c

www.rsc.org/loc

Introduction

Recent advances in cell mechanobiology demonstrated the remarkable capacity of stem and terminally differentiated cells, to sense, respond, and adjust to rapid changes in their micro-environment, collectively referred to as mechanoadaptation.^{1–6} It was demonstrated that mechanoadaptation regulates cell decision events, such as cell growth and proliferation,^{7,8} apoptosis,⁹ differentiation,^{10–13} and shape modulation.^{14,15}

Moreover, its respective regulation and dysregulation are tightly coupled to tissue health and disease states. For example, vascular endothelial cells (ECs), which form an intraluminal monolayer at blood and lymphatic vessels and act as a first line of defence for the blood-brain barrier integrity, respond to both strain and haemodynamic shear stresses. Under normal physiological conditions ECs regulate

vasodilation,¹⁶ blood anticoagulation¹⁷ and angiogenesis.¹⁸ Under conditions of reduced flow, the EC monolayer shows increased permeability, allowing low-density lipoprotein (LDL) to cross the endothelial barrier, trigger a biochemical cell-signalling cascade, and leads to the formation of atheroma, which is a precursor of atherosclerosis. As indeed verified, atheroma plucks are preferentially found close to vascular branches and curvatures where flow disturbance and irregular shear distribution occur.^{19–21}

Flow-induced mechanotransduction also relates to cancer progression and metastasis.^{22,23} Under normal conditions, venous pressure induces plasma leakage through a capillary wall and subsequent uptake by the draining lymph nodes.^{24,25} This homeostasis is disrupted in cancer.²⁶ Rapid tumour angiogenesis is characterized by aberrant and leaky vasculature,^{27,28} and with dysfunctional lymphatic vessels²⁹ and stromal cell remodelling at the tumour periphery^{30,31} results in the accumulation of high tumour interstitial fluid pressure. Cells in the tumour vicinity respond to this elevated interstitial pressure by initiating phenotypic changes, secretion of pro-invasive cytokines, and extracellular matrix remodelling, all of which promote cancer metastasis.³²

^a School of Mechanical and Manufacturing Engineering, University of New South Wales, Sydney, NSW 2052, Australia. E-mail: m.warkiani@unsw.edu.au

^b Graduate School of Biomedical Engineering, University of New South Wales, Sydney, NSW 2052, Australia

^c Australian Centre for NanoMedicine, University of New South Wales, Sydney, NSW 2052, Australia

Despite the importance of mechanotransduction and mechanoadaptation processes in normal and patho-physiology, observation of physiological flows *in situ* is impractical. Tunable flow perfusion systems³³ and rapid prototyped tissue templates,¹³ in combination with novel technological platforms to engineer emergent behavior such as self-assembly of tissue templates by patterning of cell adhesion molecules,³⁴ have enabled unprecedented control over the mechanical and chemical environment of cells. Recent advances in microfluidic technologies created powerful tools for biologists to study cellular behaviours from single- to multi-cellular organism level with improved throughput and resolution, leading to new questions and new discoveries.^{35–38} The high-throughput testing and amendable design of microfluidic systems would allow efficient assessment of various regulatory mechanisms through precise control of physical and biochemical cues at cellular and sub-cellular level.

Here we review recent advances in the development of micro-flow systems for studying behavior of adherent cells under flow. We elaborate on their suitability to generate an *in vivo* – like micromechanical environment for investigation of cellular mechanotransduction and mechanoadaptation. Under physiological conditions, cells modulate their behavior in response to their prevailing mechanochemical environment, which encompasses not only flow amplitude but also its spatial and temporal variation. In this context, it is rarely noted but should be underscored that exposure of cells to fluid flow induces both shear as well as normal (compressive and/or tensile) stresses at cell surfaces.¹⁰ Furthermore, the presence of cells themselves alters flow through fluidic devices.^{34,39} Nonetheless, it is imperative to understand the mechanical and chemical cues applied by fluidic devices while measuring cellular mechanical, mechanotransductive, and mechanoadaptive responses. Here we describe basic design considerations, in relation to pumping method, chip design, cell type used, flow validation and mechanotransduction mechanism. Major cellular structures involved in mechanosensing are also discussed briefly. Other reviews cover related topics, such as mechanobiology and microfabrication,^{40–42} pumps for microfluidic cell culture,⁴³ technical design practices for microfluidic perfusion cultures,⁴⁴ and macro and micro flow systems for studying the effect of shear stress on the endothelial cells.⁴⁵

Temporal control of flow pattern

Under physiological conditions, cells display cell-specific preferential activity based on the applied flow pattern, such as the stress amplitude and type, temporal flow variation, as well as flow directionality and its spatial variation across a cell's surface. To mimic those conditions *in vitro* an appropriate pumping method needs to be selected to offer the highest degree of control while maintaining operation simplicity.

Pumping methods are broadly grouped into active and passive pumping. Active pumping which is normally controlled by the user, has moving parts, and provides defined

control over flow conditions, while passive pumping maintains the flow without external intervention and requires less equipment for implementation; however, they are less robust than active ones.⁴⁶ Two common example of active pumping are syringe⁴⁷ and peristaltic pumps,⁴⁸ which are widely used for a variety of cell culture applications. Syringe pumps typically use a piston to push liquids out of a syringe with a defined volume, while peristaltic pumps displace the liquid by compressing and relaxing a flexible hose that is positioned between a rotating device and circular pump housing. Two other common active pumps are on-chip peristaltic pumps, operated by inflating control channels incorporated above the flow channel^{49–51} and centrifugal pumping which rely on centrifugal body forces.^{52,53} Electroosmotic pumps operate by ionized liquid under an applied external electric field.⁵⁴ Passive pumping methods include gravity-driven flow which is based on reservoir height difference⁵⁵ and osmosis-driven flow and surface tension-driven flow which rely on osmolarity difference and interfacial surface energy minimization, respectively.^{56,57}

A detailed review that compares common pumping methods in microfluidic systems is given by Byun and his colleagues.⁴³ While it summarizes the technical aspects of each method, elaboration of their respective suitability for perfusion cell cultures is helpful in the context of advancing the field of microfluidics. For example, pumps based on the surface-tension driven flow,⁵⁷ although simple to set up, are not well adjusted for long-term cell culture and do not provide adequate control over the flow rate. Pumps based on electro-osmotic flow⁵⁸ have the advantage of on-chip integration and a small footprint. However, the applied electric field required for their operation could interfere with cell functionality. In addition, the flow depends on the polar characteristics of the medium, and its flow profile deviates from the typical parabolic velocity distribution.⁵⁹ Osmosis-driven flow has the advantage of passive pumping but is limited to low flow rates⁵⁶ and potential adverse effects of osmotic gradients on cellular behaviour. For these reasons, the majority of works on adherent cells under flow rely on one of the pumping methods described in Table 1, the simplest of which is gravity-induced flow. Sellgren *et al.* demonstrated a biomimetic model of the human airway using epithelial cells, lung fibroblasts, and endothelial cells using the height difference method.⁶⁰ This approach was also used to investigated the role of neuroprotective glial cells and a multiple sclerosis drug on the Aβ toxicity of primary central nervous system cells.⁶¹ The passive nature of this system eliminates the requirement for active pumping and any moving part during operation. Its drawbacks are reduced flow control, a bulky apparatus, and the inability to create pulsatile or bidirectional flow.

Improved control over flow regimes without a substantial increase in complexity is achieved by active pumping. The majority of works use active mechanical pumps, such as a syringe or peristaltic pumps.^{62–66} In spite of their ease of operation and good adjustment to long-term cell cultures,

Table 1 Common characteristics of flow control methods

	Method	Open system	Physics of driving force	Dead volume	Setup/fabrication complexity	Temporal control over flow rate	Ref.
Unidirectional flow	Height difference	Yes	Hydrostatic pressure	Medium	Low	Low	60, 61
	Centrifugal	No	Centrifugal force, Coriolis force, Euler force	Low	High	Medium	69, 71, 73
Bidirectional and pulsatile flow	External mechanical pump (syringe/peristaltic)	No	Hydrostatic pressure	High	Low	Medium	64, 74, 62, 63, 75
	On-chip peristaltic pump	No	Hydrostatic pressure	Low	High	High	68

their limitations are the use of large residual volume and the difficulty to perform multiplexing without adding separate fluid control modules. On-chip miniaturized peristaltic pumps can overcome this by introducing pneumatically driven control channels.^{49,67} Using this method, Chen and colleagues⁶⁸ reported a microcirculatory pulsatile version of a chamber heart in a continuous culture with a small working volume of ~2–3 µl. The on-chip peristaltic pump was designed to induce flow circulation in order to mimic the phases of a heart cycle and demonstrated the importance of pulsatile flow on arterial endothelial cells. Another method to control flow is by using centrifugal forces.^{69,70} Using this approach Ren and colleagues were able to reduce *Pichia pastoris* culturing time from 8–12 h down to 2 h.⁷¹ Although limited by flow directionality and the ability to easily visualize cultured cells, it supports the use of low reagent volumes, the ability to perform multiplexing, and can potentially be interfaced with existing desktop DVD technology.⁷²

Spatial control of flow pattern

In conjunction with the selection of an appropriate pumping method to mimic a physiological flow regime, geometric and other chamber design considerations are important for spatial control of flow pattern.^{39,76} Designs that exploit the tight tolerances and accurate flow control of soft lithography are used extensively in research to investigate the effect of flow on cells. One of the simplest examples is a straight microchannel with a rectangular cross-section, driven under continuous flow. Such simple geometry was used to investigate the effects of hydrodynamic conditions on biofilm growth,⁷⁷ and the osteoblast response to fluid flow.⁷⁸ Song and colleagues combined the microchannel with microscale particle image velocimetry for *in situ* spatiotemporal mapping of flow fields around mesenchymal stem cells and discovered that the presence of cells as well as their seeding density significantly influences local flow fields.⁷⁹ This simple channel configuration was also recently used to characterize receptor–ligand adhesive interactions of P- and L-selectin.⁸⁰

In order to achieve variable flow conditions, an additional degree of control must be incorporated into the device design. For example, local increased shear stress can be introduced at the vicinity of corners, restrictions, and pillars. Due to their ability to mimic physiological conditions of spatially localized shear they are routinely used to explore the

role of fluid flow on platelet aggregation.^{81–83} Recent work that implemented these geometries with pulsatile flow found that clot height significantly increased as a result of a small reduction in trans-thrombus pressure drop.⁶⁶ Garza-Garcia and colleagues cultured Chinese hamster ovary (CHO) cells in curved channels and demonstrated an increase of monoclonal antibody production by three orders of magnitude.⁸⁴

Multichannel configuration is needed in order to perform multiplexing,^{61,85,86} as shown in Fig. 1(A). In this design, channels with different hydrodynamic resistances⁸⁷ or a single channel with a variable cross section⁸⁸ (see Fig. 1(B)) is used to rapidly scan the effect of shear stress level on cells, typically under continuous flow. Rotenberg and co-workers adopted this configuration for design of a novel 3D perfusion bioreactor to investigate the effect of different shear levels on human umbilical vein endothelial cells (HUVEC) in alginate-made scaffolds and demonstrated the influence of flow levels on ICAM1 and eNOS expression as well as cell sprouting.⁶⁴ Chau *et al.* designed a multishear microdevice to study effect of 10 different shear stress values on HUVEC cells and found that shear stress above 5 dyn cm⁻² resulted in increased secretion of von Willebrand factor.⁷⁴ Variable flow channel dimensions were also used to investigate the effect of shear stress on osteoblast proliferation, differentiation and expression of Runx2.⁸⁹

A correlation between HUVEC cells apoptosis, glucose levels, and shear flow was determined based on a novel device that combines channel connectivity and fluorescence resonance energy transfer (FRET) biosensor.⁶⁵ Modifying the shear stress within a single channel was also demonstrated by Rossi and co-workers⁸⁸ using tapered geometry with a channel cross-section that increases linearly along the flow axis. They reconstructed the topography and shear stress distribution over the surface of single endothelial cells and correlated it to the expression of the shear-responsive gene KLF2. Wang *et al.* cultured endothelial cells in a single channel with stepwise increasing widths and reported the upregulating of the tetrapeptide AcSDKP and the effect of the CA-4 drug on cytoskeleton remodelling.⁹⁰

Combining fluid flow with an additional stimulus (mechanical^{93–95} and³⁹/or chemical^{96,97}) provides another strategy to rapidly assess cell responses. For example, in the case of mechanical stimuli, as depicted in Fig. 1(C), Huh *et al.* cultured small airway epithelial cells in an air-liquid two-phase microfluidic device that models lung injury and

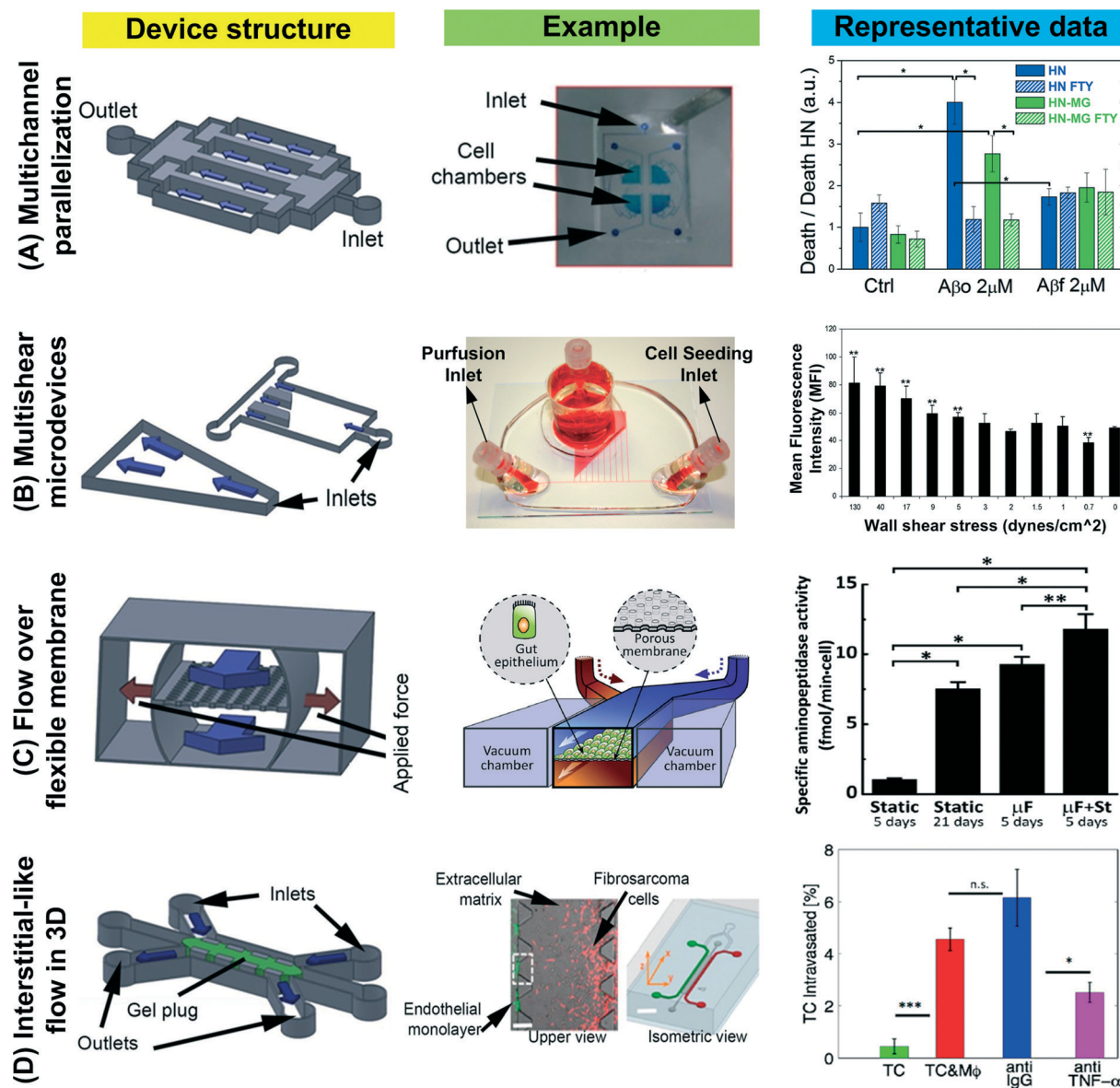


Fig. 1 Typical microfluidic flow system configurations. Blue arrows indicate flow direction in “device structure” column. (A) Multichannel configuration used for high-throughput drug screening on different populations of primary central nervous system (CNS) cells under physiological fluidic shear conditions (adapted from ref. 61). (B) Shear stress modulation based on difference in channel hydrodynamic resistance used to investigate secretion level of von-Willebrand factor (vWF) by human umbilical vein endothelial cells (HUVEC) (reproduced from ref. 74). (C) Combined flow and strain applied to cell-seeded porous membrane to mimic the human intestine (reproduced from ref. 91). On the basis of this concept, many organ-on-a-chip devices have been developed to study the physiological function of different organs such as blood vessels, lung, liver and kidney. (D) 3D microfluidic systems designed to control microenvironmental factors (e.g., cell-cell interaction, 3D ECM-like microenvironment) and perform live cell imaging while exploring the relationship between tumor cell intravasation and endothelial permeability in the context of cytokine induced endothelial cell activation and paracrine signaling loops (reprinted with permission from ref. 92).

found that propagation and rupture of liquid plugs lead to significant injury of small airway epithelial cells by generating fluid mechanical stresses.⁹⁸ Maeda and colleagues designed a microgroove structure that mimics collagen fibres and simultaneously applies cyclic tensile strain and fluid shear stress to tenocytes.⁹⁹ In another interesting study, Hegde *et al.* investigated the effect of flow-induced shear on a hepatocytes monolayer grown in collagen. The use of a porous membrane to separate the flow layer from the cell

layer improved mechanical stimuli, leading to a connected cellular network associated with higher secretion of urea and albumin. The authors also demonstrated that improved cell performance is linked to collagen secretion.¹⁰⁰ An integrated microdevice incorporating micropost array, microcontact printing and flow was used to characterize a single cell's contractile forces.⁶³

Combining flow and strain using deformable membranes helps model the epithelium found in organs, such as lungs,

blood, and lymphatic vessels. For example, a biomimetic flow system composed of two channels, separated by a porous membrane under cyclic strain was used to mimic the human gut on a chip.⁹¹ Human intestinal epithelial cells were cultured on the membrane and subjected to low shear stress ($0.02 \text{ dyne cm}^{-2}$). Under these conditions, a columnar epithelium formed, polarized, and grew into intestinal villi-like folds that displayed a high integrity barrier to small molecules compared with static cultures. Sinha *et al.* used deformable membranes to combine strain and flow in order to scan multiple strain-shear flow amplitude combinations using a multi-unit chamber chip.¹⁰¹ For this, they used a stretchable membrane sandwiched between a strain-modulating circular array of increasing diameter on one side and an array of tapered flow chambers to modulate the flow-induced shear on the other.

Introducing biochemical stimulation together with flow offers a new opportunity to investigate cellular chemotaxis and directed migration occurring at a blood vessel interface in a more controlled environment. For this, a micro-device was designed composed of a static gel plug seeded on both sides by two different cell monolayers and infused by transverse flow and a chemical gradient to mimic interstitial flow in 3D⁹² (Fig. 1(D)). This unique design successfully addressed basic questions related to the effect of interstitial flow on cell chemotaxis and activation in the case of cancer metastasis.^{102,103} Using a similar microfluidic system it was demonstrated that ECs sprouting is governed by interstitial flow in a RhoA-dependent manner⁶² and is attenuated by shear stress in a nitric oxide-dependent manner.¹⁰⁴ Interestingly, it was found that interstitial flow promotes capillary morphogenesis with localization patterns of VE-cadherin and increased FAK phosphorylation when flow is applied along a cell's basal-to-apical direction, but it displays no such behaviour for flow applied along a cell's apical-to-basal direction.¹⁰⁵ Biochemical stimuli were also recently reported by Kalashnikov and colleagues to accelerate antibiotic susceptibility testing of *staphylococcus aureus*.⁷⁵

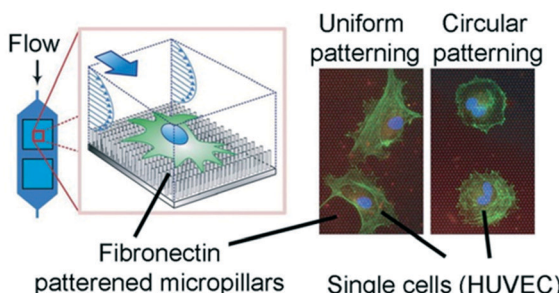
To summarize, various approaches have emerged to manipulate flow-induced stresses while modulating the geometrical configuration of the cultured cells' microenvironment. Single flow channels are used to characterize the influence of surface affinity⁸⁰ and topology modulation^{63,106} on cellular responses. This configuration requires minute amounts of reagents for operation, promotes faster cell confluence and can be used as an intermediate step towards a more complicated biochip design. However, to increase experimental efficiency, rapid and parallel screening of multiple parameters are needed, which require more sophisticated platforms. Multi-shear devices, as depicted in Fig. 1(B), can apply multiple shear stress levels simultaneously on a single chip. One major challenge for successful operation of this configuration is uniform plating of cells across the various chambers. Another limitation is perturbation of flow in adjacent channels due to flow disturbance in other channels caused by clogging or bubble formation, which can be

reduced using tapered geometry.^{88,107} Flow over a flexible (and/or permeable) membrane,¹⁰⁸ as illustrated in Fig. 1(C), is also widely used for applying multi-directional shear stress on cultured cells^{60,100,109} with more sophisticated emerging capabilities of simultaneously applying mechanical, electrical, and biochemical stimulation.¹¹⁰ Main advantages of such systems are the control over a cell's physical microenvironment by independent modulation of its temporal strain and flow-induced shear as well as the ability to position cells in a 3D architecture that mimic cell-cell interaction commonly found in the native environment.⁹⁴ On the basis of this concept, many organ-on-a-chip devices have been developed to study the physiological function of different organs such as lung,¹¹¹ bone marrow,¹¹⁰ and gut⁹¹ just to name a few. However, complex procedures for their assembly and operation limit their widespread usage in other laboratories. The configuration described in Fig. 1(D) mimics multicellular flow models with considerable operational simplicity at the expense of reduced temporal flow control. Due to its 3D configuration one of its main challenges is the accurate quantification of shear forces at the sub-cellular level using high resolution imaging, such as time-lapse confocal microscopy.^{10,62,112}

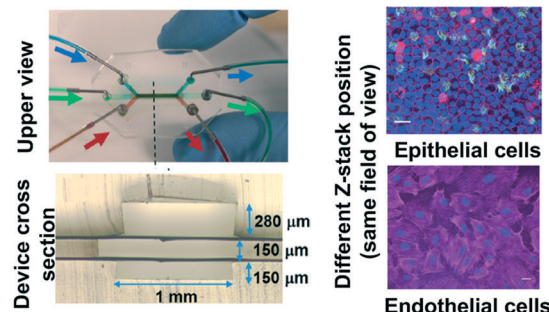
While innovative microfluidic systems will continue to be developed, we envision that hybrid systems which combine advantages of existing technologies will emerge. This will enable real-time mapping of cellular responses to the mechanical stimulus such as the stress and strain levels, and their temporal pattern together with biochemical and electrical stimulations.^{87,93,102,113,114} Fig. 2 shows few microfluidic flow systems that have been developed to investigate the biological responses of cells and tissues to various mechanical stimuli. Fig. 2(A) demonstrates the combination of micro-patterned substrates with microfluidic flow systems that could enable independent controls and modulations of fluid shear and substrate rigidity for analysis of morphological changes at the single-cell level.⁶³ Fig. 2(B) and (C) present biomimetic flow systems to model the airway⁶⁰ and cardiac tissue,⁶⁸ respectively. The former design combines a complex 3D architecture and multi-cellular culture for mimicking of the human airway mucosal microarchitecture using all primary cells, while the latter incorporated an on-chip micro-pump to generate a cardiac-like flow in a continuous culture system for *in vitro* study of vascular hemodynamics and endothelial cell responses. Fig. 2(D) showcases a unique methodology to investigate cancer cell mechanics by characterizing a single cell's response to flow acceleration.¹¹⁵

Verification of flow regimes and induced shear

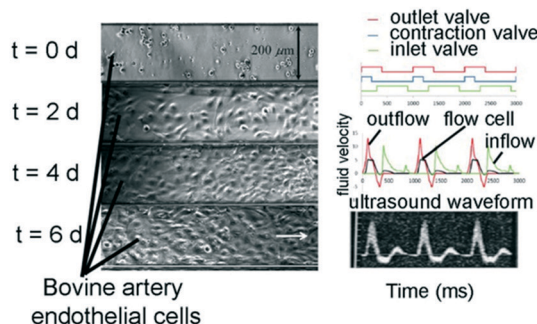
The most critical parameter to consider when designing a microfluidic flow chamber is the magnitude of shear stress applied on the cultured cells which can be approximated based on the inlet flow rate, channel geometry and fluid viscosity.⁴⁴ In practice flow irregularities can potentially affect



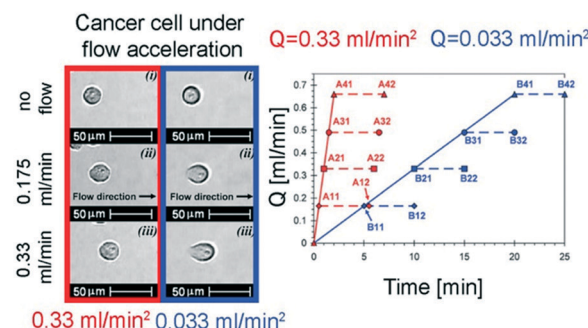
(A) Patterned micropost array



(B) Tri-culture airway biomimetic



(C) Cardiac-like flow generator



(D) Cell response under flow acceleration

Fig. 2 Selected microfluidic systems demonstrating control over temporal flow pattern, geometrical configuration, and sub-cellular microenvironment. (A) Fibronectin patterned micropost array to investigate morphological changes of HUVEC at the single-cell level (adapted and reproduced from ref. 63). (B) A biomimetic multicellular model of the human airways using tri-culture primary cells (adapted and reproduced from ref. 60). (C) Cardiac-like flow generator for long-term endothelial cell culture (adapted and reproduced from ref. 68). (D) Cancer cells under flow acceleration in a bio-functionalized microchannel (adapted and reproduced from ref. 115).

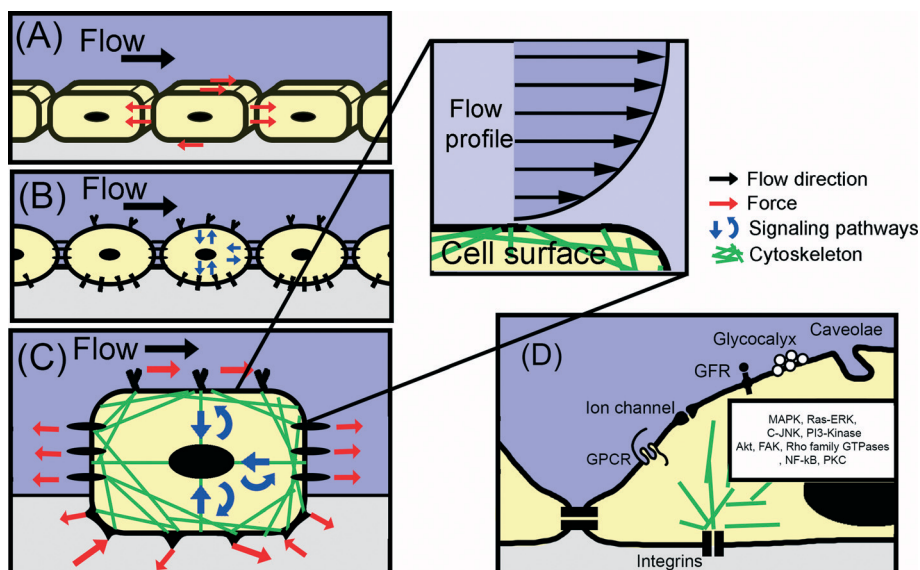


Fig. 3 Cell mechanosensing model approaches at the micro- and nano-scale. (A) A simplified engineering model where a cell is composed of a spatially uniform isotropic material subject to a stress distribution dictated by forces applied at its boundaries. Shear and tensile stresses within the cell body vary continuously between any two given points. (B) A simplified biological model in which a cell interacts with its surroundings by binding to surrounding cells, ECM, and signaling molecules which, in turn, triggers intracellular biochemical pathways. (C) A mechanosensing approach, where a cell internalizes both mechanical and biochemical signals. Forces are applied at discrete local points and are transmitted through the cell body along cytoskeletal microstructures. Cell's shape and its physical characteristics vary over time based on the applied force pattern. (d) Schematic representation of selected membrane-bound nanoscale structures involved in intracellular mechanical signaling.

this value due to multiple factors such as cell sedimentation in the vicinity of the device inlet, micro fabrication defects and the presence of micro-sensors incorporated into the devices flow channel.⁸⁷ Flow variations at the sub-cellular scale,¹¹⁶ which also depend on the seeded cell densities,⁷⁹ should also be carefully considered, as well as the fact that idealized shear stress is an approximation. The majority of microflow devices use PDMS elastomer which does not swell in water¹¹⁷ but does deforms under pressure.¹¹⁸ Gervais and colleagues have demonstrated that channel deformation is an important consideration that affects flow, especially in low aspect ratio channels with changes occurring along the stream-wise axis.¹¹⁹ Mechanical compliance of PDMS also contributes to syringe-pump driven pressure fluctuations in microchannels, which was characterized by Zeng *et al.*¹²⁰

The permeability of PDMS to gases often leads to air bubble formation.¹²¹ The presence of a single bubble can increases the wall shear stress in a liquid-perfused micro-channel by over one order of magnitude and should therefore be avoided. Air bubbles can be actively removed^{122,123} or minimized.^{39,76,95,124} In other cases, the velocity flow field is difficult to calculate due to flow acceleration around edges and close to the microchannel interconnections. For this, the Navier–Stokes equations are solved using computational fluid dynamics for the velocity field distribution which is then used to derive the wall shear stress.^{66,84,106} Ideally, these simulations should be verified by measuring the flow velocity field based on microparticle displacement. The most widely used method is micro-scale Particle Image Velocimetry (μ -PIV).^{68,99,125} In this method tracer micro-scale particles in the flow are recorded at two instants of time and from the change of the particle distribution over time, the flow motion is determined.¹²⁶ At sub-cellular scale μ -PIV is limited by the smaller field of view and the image acquisition rate. A complementary method to overcome this quantifies the point displacements of microbeads coated with a protein that targets the glycoproteins on the cell membrane.¹⁰ Using point measurement and assuming a Poiseuille flow, Booth and colleagues demonstrated novel flow validation at specific point by on-chip integration of a micro-flow sensor array.⁸⁷

Shear flow and cell mechanotransduction

Shear stress in a flow results from intermolecular friction forces between two liquid layers slipping over each other. In Poiseuille flow, the velocity field is derived by solving the Navier–Stokes equations for the case of steady incompressible laminar flow while assuming constant pressure gradient along an axisymmetric pipe axis and using a no-slip condition at the wall surface (see Fig. 3(C)). In this configuration, the shear stress is maximal at the wall interface where cells are typically cultured. Alternatively, rectangular, rather than circular cross section are commonly used to estimate shear stress on adherent cells in microfluidic devices at the cell–liquid interface.^{109,115,127} Nevertheless, these computed

values should be regarded as an approximation only. In practice, a cell's surface is neither smooth nor uniform (Fig. 3). Within its lipid membrane are incorporate membrane-bound as well as transmembrane proteins that form complex structures such as protrusions (cilia), pocket-like invaginations (caveolae), selective pores (ion channels) and long-chain molecules (proteoglycans and glycosaminoglycans). Their role in flow-induced stress is well recognized^{128–131} but the precise elucidation of each mechanism is challenging due to their sub-micrometer scale. Below, we briefly describe key cellular structures involved in mechanosensing. Due to the large body of literature on ECs and their ubiquitous role in flow-induced mechanosensing they are used here as a model.

Ion channels

The ion channels are categorized as the fastest transducers of mechanical stress in cells. These channels are embedded in the plasma membrane of cells and are therefore sensitive to both cellular-scale and tissue-scale stresses. It has been determined that several flow-responsive ion channels are involved in sensing shear stress flow. The serial event of activation begins with the inward rectifying K^+ channels and outward rectifying Cl^- channels. The K^+ flux initiates the Ca^{2+} entry into the cells, which activates two shear stress-dependent ion channels, P2X purinoceptors and transient receptor potential channels. Na^+ channels have also been involved in shear stress sensing and were detected in mammalian endothelial cells. Na^+ influx was found to inhibit shear-induced modulation by ERK1/2 activation.

Caveolae

Caveolae in endothelial cells act with ion channels, calcium signalling, and ATP (adenosine triphosphate) synthase and have been observed to induce calcium response initiation at the caveolae sites. This makes the caveolae sites a potential candidate for shear stress sensing.

G-protein coupled receptors

G-protein coupled receptors (GPCR) are involved in mechanotransduction of shear stress. These receptors are ligand-independent and are activated by inflammatory mediator bradykinin B2 through a conformational change. In the absence of their receptor, purified GPCR are activated *via* shear stress, indicating that their activation can also occur in a shear-stress independent manner.

Tyrosine kinase

Similar to GPCR, shear stress can also activate tyrosine kinase receptors (VEGFR2, TIE2) independent of their ligand and through phosphorylation.^{132–134} The phosphorylation of VEGFR2 can also occur through the shear stress-induced ATP release from the caveolae and lipid raft-bound ATP synthase.¹³⁵ Activation of tyrosine kinase initiates several

signalling pathways in cells such as erk, c-Jun N-terminal kinase (JNK), PI3 kinase, and AKT1.

Sensing of the shear stress by cells

Cell adhesion molecules

A variety of adhesion molecules have been associated with shear stress sensing. It has been found that integrins are activated by shear stress, and this activation affects the intracellular Ras-ERK signalling pathway.^{136,137} It is also found that integrins transmit shear stress signals to the cytoskeleton.^{138,139} The Ras-ERK signalling pathway is also activated through shear stress – induced phosphorylation of the platelet EC adhesion molecule (PECAM-1), located at the cell junctions.¹⁴⁰

Glycocalyx

Glycocalyx is a network of transmembrane proteins that protrude into the arterial lumen and are coiled under a no flow condition. Increased flow unfolds glycocalyx along the flow direction, mediates conformational changes of the protein, and increases Na^+ ion binding sites that initiate signalling pathways.^{141,142} It has also been postulated that glycocalyx may transmit shear stress through its core protein glycan to the caveolae,¹⁴³ where phosphorylation of eNOS takes place through the Src pathway.¹⁴⁴

Primary cilia

It is believed that bending the cilia at the surface of ECs increases the permeability of the ion channels, which leads to the flux of the Ca^{2+} and calcium-induced signal transduction.¹⁴⁵ The glycoproteins polycystin-1 and -2, which are localized on the primary cilia of the endothelial cells, are involved in shear stress sensing in both mouse and human, which subsequently activates calcium-dependent pathways.^{146,147}

Intracellular response to shear stress

Shear stress activates a number of intracellular biochemical pathways, such as focal adhesion kinase (FAK), Rho family GTPases, PI3-kinase, mitogen-activated protein kinases (MAPKs), protein kinase C (PKC), and nuclear factor- κ B (NF- κ B).^{148–153} Shear stress alters the expression of more than 3,000 genes in endothelial cells. Generally, shear stress induces the expression of genes that impact growth factors, adhesion molecules, vasoactive substances, endogenous anti-oxidants, coagulation factors, and chemoattractants. mRNA transcription of a variety of growth factors, such as platelet-derived growth factors-A and -B, basic fibroblast growth factors, heparin-binding epidermal growth factor-like growth factor and transforming growth factor- β , increases in ECs in response to shear stress. Conversely, it is shown that the gene expression of adhesion molecules such as vascular adhesion molecule-1 (VCAM-1) is decreased in response to steady shear stress, leading to the decrease in leukocyte adhesion to the vascular wall. An increase in the production of vasodilator

nitric oxide (NO) and prostacyclin has been observed after the exposure of endothelial cells to steady shear stress. Anti-thrombotic proteins, such as tissue plasminogen activator, thrombomodulin, and cyclooxygenase-2 are also upregulated in response to shear stress as well as the expressions of superoxide dismutase (SOD) genes. This leads to an increase in the capacity to mitigate reactive oxygen species.

Cell type and shear flow pattern

Spatial and temporal flow velocity field distributions in organs vary due to difference in cavity dimensions, driving pressure generating the flow, and the surrounding tissue's mechanical compliance. This results in distinct flow patterns, which, together with the native cell responses, regulate both single and multicellular processes, such as angiogenesis,^{154–156} lymph transport and function,^{157,158} and stem cell differentiation (Fig. 4).^{159,160} Microfluidic devices therefore aim to emulate flow condition for each cell type, yet retain as many general features of native tissue. Cell types cultured in microflow devices include endothelial cells, stem cells, fibroblasts, osteoblasts, smooth muscle cells, hepatocytes, cancer cells, neuronal cells and bacteria. Table 2 classifies these works based on the cell-type and flow pattern.

Due to their high sensitivity to flow as well as the large body of literature, the majority of works use endothelial cells, specifically human umbilical vein endothelial cells (HUVEC).^{161,162} The shear stress amplitude used for ECs were typically in the range of tens of dyn cm^{-2} to match physiological conditions, but amplitudes of up to 130 dyn cm^{-2} were also reported.⁷⁴ The lowest shear stress in Table 2 was continuous flow applied on osteoprogenitor cells (15×10^{-3} – $4.1 \times 10^{-3} \text{ dyn cm}^{-2}$) and was highest in pulsatile flow on fibroblasts (up to $1.6 \times 10^{-3} \text{ dyn cm}^{-2}$). Applied flow duration typically ranges between a few hours to four days but was also applied for up to 14 days (ref. 61) or more.¹⁶³

Cell characterization techniques

Characterizing cell response in microfluidic systems is challenging due to limited access to the cultured cells for staining and lysis as well as further complexity when probing 3D configurations using more involved imaging and analysis techniques. A variety of methods are available to monitor both real-time and end-point cell activity under flow. The majority of the works rely on either simple phase-contrast imaging,^{86,170} or fluorescent tagging followed by fluorescent⁶⁶ or confocal⁷⁷ microscopy. Phase contrast microscopy is extensively used to characterize cell-scale response by tracking a cell's deformation,^{87,115,164} surface area,^{84,115} orientation angle,^{87,109,116,164} adhesion,^{80,116,163} migration⁹³ and proliferation.⁶⁸ It provides a simple, non-invasive optical characterization but offers limited information about the underlying mechanisms involved. More details can be obtained by immunostaining^{105,106} which identifies the involvement and localization of specific mechanosensitive elements such as

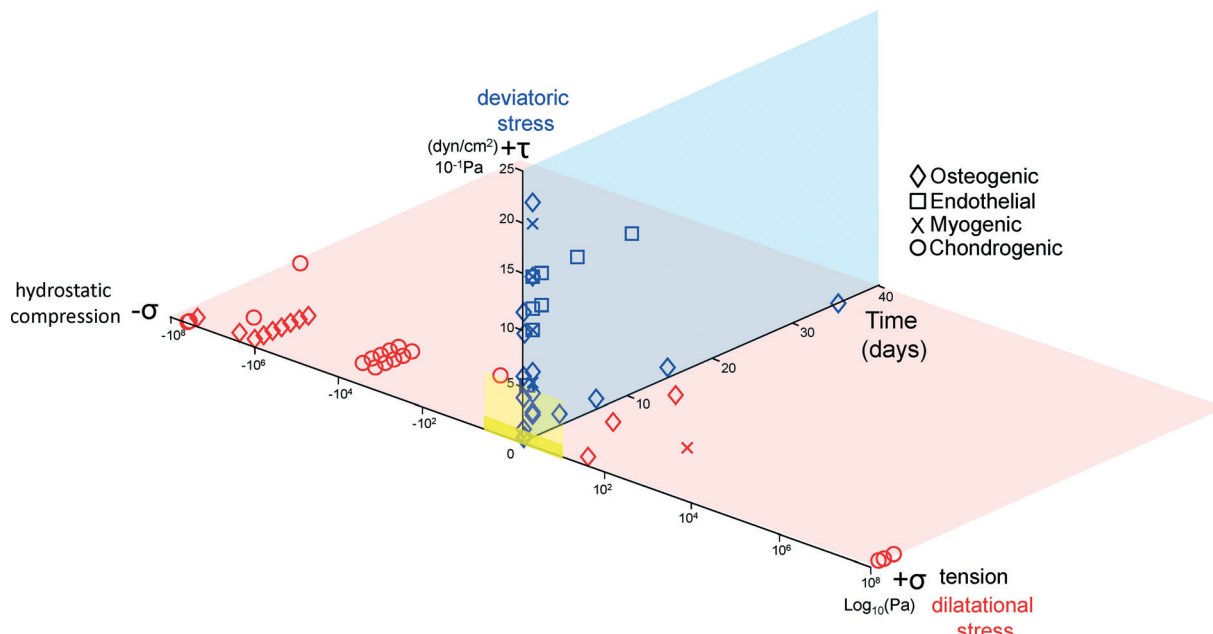


Fig. 4 Characteristic magnitudes and time domains of mechanical signals applied in studies of multipotent cell differentiation. Reproduced with permission from ref. 39, 76.

Table 2 Cell types used for flow in microdevices, sorted by cell type and flow pattern

	Cell type	Shear stress range [dyn cm⁻²]	Applied flow duration	Ref.
Continuous	Endothelial cells	0–20	2 h–5 days	60, 62–64, 90, 104, 106, 109, 164–167
	Stem cells	0–26	6 h–3 days	94, 168
	Fibroblasts, osteoprogenitor cells, smooth muscle cells	0–20	Up to 48 h	69, 89, 93
	Cancer cells	0.25–3	Up to 7 days	80, 103, 169
	Neuronal, hepatocytes, tenocytes	—	1 h–14 days	61, 99, 100
	Bacterial	20–60	1 h, 24 h	71, 75
Pulsatile	Endothelial cells	15–30	12 h–6 days	65, 85, 87, 105, 125, 68, 88
	Cancer cells	0.3–7	5–30 days	114, 163
	Fibroblasts, osteoblasts	1–1600, 0–20	30 min, 8 h	78, 116
Pulsed	Epithelial cells	0.02–100	7 days	91, 98
	Stem cells (see also recent compilation of all stem cell studies to date, Fig. 4 (ref. 13))	—	6 days	86
Monotonically increasing	Bacterial	30–90	80 h	77
	Prostate and breast cancer cell lines	—	15 min	115

VE-cadherin and actin.^{109,125} Another important tool, albeit less frequently used in micro-flow devices, is nucleic acid quantification.¹⁶⁹ It quantifies gene expression at specific time point. Nevertheless, due to cell averaging over the harvested cells, it is limited to quantification of single experimental conditions. Both nucleic acid analysis and immunostaining of intracellular proteins sacrifice the cells and therefore cannot provide real-time data. Due to these limitations, complementary methods are used to probe real-time cell activity in micro-flow systems. These include biomolecules uptake and secretion,^{84,100,125} live cell labelling,^{114,171,172} trans-endothelial electrical resistance assay (TEER),^{87,173} cell transfection^{65,164} and cell permeability assays.^{87,114}

Multichannel analysis that tracks a cell's morphology, subcellular microstructures and cell functionality simultaneously with high temporal resolution is therefore desirable.

Conclusions and future directions

The identification of flow as a key cellular mechanoregulator has increased the demand for state-of-the-art micro-flow systems that accurately mimic the physicochemical conditions found in a cell's native microenvironment. In this review, we presented the recent progress in microfluidic flow systems for this purpose. We discussed device design considerations,

typical cell systems used, and sub-cellular mechanosensing mechanisms.

In spite of considerable progress in the field, there are several unmet challenges, one of which is the need to establish a reliable knowledge base that correlates flow velocity amplitude and its temporal pattern to cell activated signalling pathways and activity. Detailed mechanical mapping of this type is highly complicated due to the multiple factors involved, such as cell type used, cellular heterogeneity, chemical cues introduced, and a cell's state. Nevertheless, its realization is becoming a first step towards systematic mechanical cell profiling and the emergence of new therapeutic strategies.

Within this shared effort, microfluidics plays a dominant role due to its superior flow-handling capabilities, multiplexing, and its capacity to easily integrate novel complementary modules to account for various microenvironment cues. Due to the multidimensional space that needs to be scanned, complex flow-system design and operation is justified. However, in the case of a relatively well-characterized cell response, simplicity and point-of-care capabilities are still highly desirable. One of the main barriers towards further chip miniaturization is the inadequacy of pumping techniques. For example, commercial peristaltic or syringe pumps are simple to operate and offer good flow control but are bulky, and makes their system integration difficult. On-chip peristaltic pumps are more compact, yet demand complex operation and fabrication. Centrifugation-based pumping, which relies on fluid's inertial properties, rather than pressure to induce flow, offers the potential to overcome these limitations, but is restricted to unidirectional flow. A commercially available, miniaturized, ready-to-use pumping module with capability of producing a wide range of flow rates and flow patterns could offer significant benefits to meet this need. Once these challenges are met, simple portable flow systems may be in high demand due to their potential to serve as a new personalized diagnostic tool, especially in cardiovascular-associated diseases and their early prevention.

Another issue, which is common to many microfluidic cell culturing systems, is the difficulty to access and retrieve cultured cells. In the case of macro-scale flow systems, such as the parallel-plate flow chamber, the system can be dismantled to allow access to cultured cells. However, in most microfluidic devices, once the cells are introduced into the system, cell retrieval for downstream analysis is non-trivial.

This is important for flow-based devices in order to fully exploit chip multiplexing, since biomarkers alone preclude an in-depth cell analysis. Methods that use increased shear flow to mechanically detach cells can partially address this problem. However, a more robust approach is yet to be demonstrated.

In the past, the majority of flow systems were used to test the effect of flow on endothelial cells. Recently, with the advent of new discoveries in mechanobiology, there is a growing interest in other cell systems as well, such as cancer and stem cells. This should extend to include a growing number

of cell types. Micro-flow systems are ideally suited for these ventures. Mechanobiology is a relatively young research field that continuously improves our fundamental understanding of cell biology. New discoveries have the potential to extend therapeutic strategies in the case of diseases caused by faulty mechanotransduction pathways. Microfluidic flow-based platforms have established themselves as a central player within this collective effort and are expected to continue to lead the field to new discoveries and innovative applications.

References

- 1 E. Tzima, M. Irani-Tehrani, W. B. Kiosses, E. Dejana, D. A. Schultz, B. Engelhardt, G. Cao, H. DeLisser and M. A. Schwartz, *Nature*, 2005, **437**, 426–431.
- 2 D. Mitrossilis, J. Fouchard, A. Guiroy, N. Desprat, N. Rodriguez, B. Fabry and A. Asnacios, *Proc. Natl. Acad. Sci. U. S. A.*, 2009, **106**, 18243–18248.
- 3 M. Prager-Khoutorsky, A. Lichtenstein, R. Krishnan, K. Rajendran, A. Mayo, Z. Kam, B. Geiger and A. D. Bershadsky, *Nat. Cell Biol.*, 2011, **13**, 1457–1465.
- 4 E. J. Anderson, T. D. Falls, A. M. Sorkin and M. L. Knothe Tate, *Biomed. Eng. Online*, 2006, **5**, 27.
- 5 S. H. McBride, T. Falls and M. L. Knothe Tate, *Tissue Eng., Part A*, 2008, **14**, 1573–1580.
- 6 M. L. Knothe Tate, T. D. Falls, S. H. McBride, R. Atit and U. R. Knothe, *Int. J. Biochem. Cell Biol.*, 2008, **40**, 2720–2738.
- 7 R. Singhvi, A. Kumar, G. P. Lopez, G. N. Stephanopoulos, D. I. Wang, G. M. Whitesides and D. E. Ingber, *Science*, 1994, **264**, 696–698.
- 8 P. P. Provenzano and P. J. Keely, *J. Cell Sci.*, 2011, **124**, 1195–1205.
- 9 C. S. Chen, M. Mrksich, S. Huang, G. M. Whitesides and D. E. Ingber, *Science*, 1997, **276**, 1425–1428.
- 10 M. J. Song, S. M. Brady-Kalnay, S. H. McBride, P. Phillips-Mason, D. Dean and M. L. Knothe Tate, *PLoS One*, 2012, **7**, e43601.
- 11 C. J. Flaim, S. Chien and S. N. Bhatia, *Nat. Methods*, 2005, **2**, 119–125.
- 12 A. J. Engler, S. Sen, H. L. Sweeney and D. E. Discher, *Cell*, 2006, **126**, 677–689.
- 13 M. J. Song, D. Dean and M. L. Knothe Tate, *Biomaterials*, 2013, **34**, 5766–5775.
- 14 K. Keren, Z. Pincus, G. M. Allen, E. L. Barnhart, G. Marriott, A. Mogilner and J. A. Theriot, *Nature*, 2008, **453**, 475–480.
- 15 Y. Shao, J. M. Mann, W. Chen and J. Fu, *Integr. Biol.*, 2014, **6**, 300–311.
- 16 L. J. Ignarro, G. M. Buga, K. S. Wood, R. E. Byrns and G. Chaudhuri, *Proc. Natl. Acad. Sci. U. S. A.*, 1987, **84**, 9265–9269.
- 17 C. T. Esmon, *Science*, 1987, **235**, 1348–1352.
- 18 D. H. Ausprung and J. Folkman, *Microvasc. Res.*, 1977, **14**, 53–65.
- 19 J. J. Chiu, S. Usami and S. Chien, *Ann. Med.*, 2009, **41**, 19–28.

- 20 D. P. Zarins Ck Fau - Giddens, B. K. Giddens Dp Fau - Bharadvaj, V. S. Bharadvaj Bk Fau - Sotturai, R. F. Sotturai Vs Fau - Mabon, S. Mabon Rf Fau - Glagov and S. Glagov, *Circ. Res.*, 1983, **53**, 502–514.
- 21 C. Hahn and M. A. Schwartz, *Nat. Rev. Mol. Cell Biol.*, 2009, **10**, 53–62.
- 22 A. B. Ariffin, P. F. Forde, S. Jahangeer, D. M. Soden and J. Hinchion, *Cancer Res.*, 2014, **74**, 2655–2662.
- 23 C. H. Heldin, K. Rubin, K. Pietras and A. Ostman, *Nat. Rev. Cancer*, 2004, **4**, 806–813.
- 24 J. M. Rutkowski and M. A. Swartz, *Trends Cell Biol.*, 2007, **17**, 44–50.
- 25 U. H. von Andrian and T. R. Mempel, *Nat. Rev. Immunol.*, 2003, **3**, 867–878.
- 26 A. C. Shieh, H. A. Rozansky, B. Hinz and M. A. Swartz, *Cancer Res.*, 2011, **71**, 790–800.
- 27 H. Maeda, H. Nakamura and J. Fang, *Adv. Drug Delivery Rev.*, 2013, **65**, 71–79.
- 28 J. Fang, H. Nakamura and H. Maeda, *Adv. Drug Delivery Rev.*, 2011, **63**, 136–151.
- 29 P. Saharinen, T. Tammela, M. J. Karkkainen and K. Alitalo, *Trends Immunol.*, 2004, **25**, 387–395.
- 30 R. Kalluri and M. Zeisberg, *Nat. Rev. Cancer*, 2006, **6**, 392–401.
- 31 G. S. Karagiannis, T. Poutahidis, S. E. Erdman, R. Kirsch, R. H. Riddell and E. P. Diamandis, *Mol. Cancer Res.*, 2012, **10**, 1403–1418.
- 32 A. C. Shieh and M. A. Swartz, *Phys. Biol.*, 2011, **8**, 015012.
- 33 Y. J. Blinder, D. J. Mooney and S. Levenberg, *Curr. Opin. Chem. Eng.*, 2014, **3**, 56–61.
- 34 S. F. Evans, D. Docheva, A. Bernecker, C. Colnot, R. P. Richter and M. L. Knothe Tate, *Biomaterials*, 2013, **34**, 1878–1887.
- 35 E. W. Majid and C. T. Lim, *Microfluidic Platforms for Human Disease Cell Mechanics Studies*, Springer, 2013.
- 36 V. Lecault, M. Vaninsberghe, S. Sekulovic, D. J. Knapp, S. Wohrer, W. Bowden, F. Viel, T. McLaughlin, A. Jarandehei, M. Miller, D. Falconnet, A. K. White, D. G. Kent, M. R. Copley, F. Taghipour, C. J. Eaves, R. K. Humphries, J. M. Piret and C. L. Hansen, *Nat. Methods*, 2011, **8**, 581–586.
- 37 C. Lok, *Nature*, 2015, **522**, 270–273.
- 38 M. E. Warkiani, B. L. Khoo, D. S.-W. Tan, A. A. S. Bhagat, W.-T. Lim, Y. S. Yap, S. C. Lee, R. A. Soo, J. Han and C. T. Lim, *Analyst*, 2014, **139**, 3245–3255.
- 39 A. M. Sorkin, K. C. Dee and M. L. Knothe Tate, *Am. J. Physiol.*, 2004, **287**, C1527–1536.
- 40 D. H. Kim, P. K. Wong, J. Park, A. Levchenko and Y. Sun, *Annu. Rev. Biomed. Eng.*, 2009, **11**, 203–233.
- 41 W. J. Polacheck, R. Li, S. G. Uzel and R. D. Kamm, *Lab Chip*, 2013, **13**, 2252–2267.
- 42 J. Rajagopalan and M. T. Saif, *J. Micromech. Microeng.*, 2011, **21**, 54002–54012.
- 43 C. K. Byun, K. Abi-Samra, Y. K. Cho and S. Takayama, *Electrophoresis*, 2014, **35**, 245–257.
- 44 L. Kim, Y. C. Toh, J. Voldman and H. Yu, *Lab Chip*, 2007, **7**, 681–694.
- 45 E. W. Young and C. A. Simmons, *Lab Chip*, 2010, **10**, 143–160.
- 46 D. Huh, J. H. Bahng, Y. Ling, H. H. Wei, O. D. Kripfgans, J. B. Fowlkes, J. B. Grotberg and S. Takayama, *Anal. Chem.*, 2007, **79**, 1369–1376.
- 47 N. Korin, A. Bransky, U. Dinnar and S. Levenberg, *Lab Chip*, 2007, **7**, 611–617.
- 48 W. Zhang, Y. Gu, Y. Hao, Q. Sun, K. Konior, H. Wang, J. Zilberberg and W. Y. Lee, *Lab Chip*, 2015, **15**, 2854–2863.
- 49 M. A. Unger, H. P. Chou, T. Thorsen, A. Scherer and S. R. Quake, *Science*, 2000, **288**, 113–116.
- 50 S. Vyawahare, S. Sitaula, S. Martin, D. Adalian and A. Scherer, *Lab Chip*, 2008, **8**, 1530–1535.
- 51 J. F. Zhong, Y. Chen, J. S. Marcus, A. Scherer, S. R. Quake, C. R. Taylor and L. P. Weiner, *Lab Chip*, 2008, **8**, 68–74.
- 52 D. Mark, T. Metz, S. Haeberle, S. Lutz, J. Ducree, R. Zengerle and F. von Stetten, *Lab Chip*, 2009, **9**, 3599–3603.
- 53 F. Schwemmer, T. Hutzenlaub, D. Buselmeier, N. Paust, F. von Stetten, D. Mark, R. Zengerle and D. Kosse, *Lab Chip*, 2015, **15**, 3250–3258.
- 54 J. S. Paustian, A. J. Pascall, N. M. Wilson and T. M. Squires, *Lab Chip*, 2014, **14**, 3300–3312.
- 55 M. Marimuthu and S. Kim, *Anal. Biochem.*, 2013, **437**, 161–163.
- 56 J. Y. Park, C. M. Hwang, S. H. Lee and S. H. Lee, *Lab Chip*, 2007, **7**, 1673–1680.
- 57 E. Berthier and D. J. Beebe, *Lab Chip*, 2007, **7**, 1475–1478.
- 58 H. Lakhotiya, K. Mondal, R. K. Nagarale and A. Sharma, *RSC Adv.*, 2014, **4**, 28814–28821.
- 59 R. J. Yang, L. M. Fu and Y. C. Lin, *J. Colloid Interface Sci.*, 2001, **239**, 98–105.
- 60 K. L. Sellgren, E. J. Butala, B. P. Gilmour, S. H. Randell and S. Grego, *Lab Chip*, 2014, **14**, 3349–3358.
- 61 A. Ruiz, P. Joshi, R. Mastrangelo, M. Francolini, C. Verderio and M. Matteoli, *Lab Chip*, 2014, **14**, 2860–2866.
- 62 J. W. Song, J. Daubriac, J. M. Tse, D. Bazou and L. L. Munn, *Lab Chip*, 2012, **12**, 5000–5006.
- 63 R. H. Lam, Y. Sun, W. Chen and J. Fu, *Lab Chip*, 2012, **12**, 1865–1873.
- 64 M. Y. Rotenberg, E. Ruvinov, A. Armoza and S. Cohen, *Lab Chip*, 2012, **12**, 2696–2703.
- 65 J. Q. Yu, X. F. Liu, L. K. Chin, A. Q. Liu and K. Q. Luo, *Lab Chip*, 2013, **13**, 2693–2700.
- 66 R. W. Muthard and S. L. Diamond, *Lab Chip*, 2013, **13**, 1883–1891.
- 67 I. E. Araci and S. R. Quake, *Lab Chip*, 2012, **12**, 2803–2806.
- 68 H. Chen, J. Cornwell, H. Zhang, T. Lim, R. Resurreccion, T. Port, G. Rosengarten and R. E. Nordon, *Lab Chip*, 2013, **13**, 2999–3007.
- 69 D. I. Walsh III, G. J. Sommer, U. Y. Schaff, P. S. Hahn, G. J. Jaffe and S. K. Murthy, *Lab Chip*, 2014, **14**, 2673–2680.
- 70 G. Wang, H. P. Ho, Q. Chen, A. K. Yang, H. C. Kwok, S. Y. Wu, S. K. Kong, Y. W. Kwan and X. Zhang, *Lab Chip*, 2013, **13**, 3698–3706.
- 71 Y. Ren, L. M. Chow and W. W. Leung, *Biomed. Microdevices*, 2013, **15**, 321–337.

- 72 X. Li, S. Weng, B. Ge, Z. Yao and H. Z. Yu, *Lab Chip*, 2014, **14**, 1686–1694.
- 73 R. Gorkin, J. Park, J. Siegrist, M. Amasia, B. S. Lee, J. M. Park, J. Kim, H. Kim, M. Madou and Y. K. Cho, *Lab Chip*, 2010, **10**, 1758–1773.
- 74 L. Chau, M. Doran and J. Cooper-White, *Lab Chip*, 2009, **9**, 1897–1902.
- 75 M. Kalashnikov, J. C. Lee, J. Campbell, A. Sharon and A. F. Sauer-Budge, *Lab Chip*, 2012, **12**, 4523–4532.
- 76 E. J. Anderson and M. L. Knothe Tate, *Biomed. Eng. Online*, 2007, **6**, 46.
- 77 J. Kim, H. S. Kim, S. Han, J. Y. Lee, J. E. Oh, S. Chung and H. D. Park, *Lab Chip*, 2013, **13**, 1846–1849.
- 78 B. Roy, T. Das, D. Mishra, T. K. Maiti and S. Chakraborty, *Integr. Biol.*, 2014, **6**, 289–299.
- 79 M. J. Song, D. Dean and M. L. Knothe Tate, *PLoS One*, 2010, **5**.
- 80 Z. Tong, L. S. Cheung, K. J. Stebe and K. Konstantopoulos, *Integr. Biol.*, 2012, **4**, 847–856.
- 81 W. S. Nesbitt, E. Westein, F. J. Tovar-Lopez, E. Tolouei, A. Mitchell, J. Fu, J. Carberry, A. Fouras and S. P. Jackson, *Nat. Med.*, 2009, **15**, 665–673.
- 82 M. Li, D. N. Ku and C. R. Forest, *Lab Chip*, 2012, **12**, 1355–1362.
- 83 E. Westein, A. D. van der Meer, M. J. Kuijpers, J. P. Frimat, A. van den Berg and J. W. Heemskerk, *Proc. Natl. Acad. Sci. U. S. A.*, 2013, **110**, 1357–1362.
- 84 L. D. Garza-García, E. García-López, S. Camacho-León, M. del Refugio Rocha-Pizaña, F. López-Pacheco, J. López-Meza, D. Araiz-Hernández, E. J. Tapia-Mejía, G. Trujillo-de Santiago, C. A. Rodríguez-González and M. M. Alvarez, *Lab Chip*, 2014, **14**, 1320–1329.
- 85 P. L. Voyvodic, D. Min and A. B. Baker, *Lab Chip*, 2012, **12**, 3322–3330.
- 86 S. Giulitti, E. Magrofuoco, L. Prevedello and N. Elvassore, *Lab Chip*, 2013, **13**, 4430–4441.
- 87 R. Booth, S. Noh and H. Kim, *Lab Chip*, 2014, **14**, 1880–1890.
- 88 M. Rossi, R. Lindken, B. P. Hierck and J. Westerweel, *Lab Chip*, 2009, **9**, 1403–1411.
- 89 W. Yu, H. Qu, G. Hu, Q. Zhang, K. Song, H. Guan, T. Liu and J. Qin, *PLoS One*, 2014, **9**, e89966.
- 90 L. Wang, Z. L. Zhang, J. Wdzieczak-Bakala, D. W. Pang, J. Liu and Y. Chen, *Lab Chip*, 2011, **11**, 4235–4240.
- 91 H. J. Kim, D. Huh, G. Hamilton and D. E. Ingber, *Lab Chip*, 2012, **12**, 2165–2174.
- 92 I. K. Zervantonakis, S. K. Hughes-Alford, J. L. Charest, J. S. Condeelis, F. B. Gertler and R. D. Kamm, *Proc. Natl. Acad. Sci. U. S. A.*, 2012, **109**, 13515–13520.
- 93 S. Song, H. Han, U. H. Ko, J. Kim and J. H. Shin, *Lab Chip*, 2013, **13**, 1602–1611.
- 94 W. Zheng, B. Jiang, D. Wang, W. Zhang, Z. Wang and X. Jiang, *Lab Chip*, 2012, **12**, 3441–3450.
- 95 A. M. Sorkin, K. C. Dee and M. L. K. Tate, *Am. J. Physiol.*, 2004, **287**, C1527–C1536.
- 96 C. Kim, J. Kasuya, J. Jeon, S. Chung and R. D. Kamm, *Lab Chip*, 2015, **15**, 301–310.
- 97 B. Kuczenski, W. C. Ruder, W. C. Messner and P. R. Leduc, *PLoS One*, 2009, **4**, e4847.
- 98 D. Huh, H. Fujioka, Y. C. Tung, N. Futai, R. Paine, 3rd, J. B. Grotberg and S. Takayama, *Proc. Natl. Acad. Sci. U. S. A.*, 2007, **104**, 18886–18891.
- 99 E. Maeda, Y. Hagiwara, J. H. Wang and T. Ohashi, *Biomed. Microdevices*, 2013, **15**, 1067–1075.
- 100 M. Hegde, R. Jindal, A. Bhushan, S. S. Bale, W. J. McCarty, I. Golberg, O. B. Usta and M. L. Yarmush, *Lab Chip*, 2014, **14**, 2033–2039.
- 101 R. Sinha, S. Le Gac, N. Verdonschot, A. van den Berg, B. Koopman and J. Rouwkema, *Lab Chip*, 2015, **15**, 429–439.
- 102 J. Kalchman, S. Fujioka, S. Chung, Y. Kikkawa, T. Mitaka, R. Kamm, K. Tanishita and R. Sudo, *Microfluid. Nanofluid.*, 2013, **14**, 969–981.
- 103 W. J. Polacheck, A. E. German, A. Mammoto, D. E. Ingber and R. D. Kamm, *Proc. Natl. Acad. Sci. U. S. A.*, 2014, **111**, 2447–2452.
- 104 J. W. Song and L. L. Munn, *Proc. Natl. Acad. Sci. U. S. A.*, 2011, **108**, 15342–15347.
- 105 V. Vickerman and R. D. Kamm, *Integr. Biol.*, 2012, **4**, 863–874.
- 106 E. M. Frohlich, X. Zhang and J. L. Charest, *Integr. Biol.*, 2012, **4**, 75–83.
- 107 J. K. Tsou, R. M. Gower, H. J. Ting, U. Y. Schaff, M. F. Insana, A. G. Passerini and S. I. Simon, *Microcirculation*, 2008, **15**, 311–323.
- 108 M. E. Warkiani, C.-P. Lou and H.-Q. Gong, *Biomicrofluidics*, 2011, **5**, 036504.
- 109 X. Y. Wang, Z. H. Jin, B. W. Gan, S. W. Lv, M. Xie and W. H. Huang, *Lab Chip*, 2014, **14**, 2709–2716.
- 110 A. Pavesi, G. Adriani, M. Rasponi, I. K. Zervantonakis, G. B. Fiore and R. D. Kamm, *Sci. Rep.*, 2015, **5**, 11800.
- 111 D. Huh, B. D. Matthews, A. Mammoto, M. Montoya-Zavala, H. Y. Hsin and D. E. Ingber, *Science*, 2010, **328**, 1662–1668.
- 112 A. Lesman, J. Notbohm, D. A. Tirrell and G. Ravichandran, *J. Cell Biol.*, 2014, **205**, 155–162.
- 113 Y. Xiao, B. Zhang, H. Liu, J. W. Miklas, M. Gagliardi, A. Pahnke, N. Thavandiran, Y. Sun, C. Simmons, G. Keller and M. Radisic, *Lab Chip*, 2014, **14**, 869–882.
- 114 S. Kim, H. Lee, M. Chung and N. L. Jeon, *Lab Chip*, 2013, **13**, 1489–1500.
- 115 L. S. Cheung, X. Zheng, A. Stopa, J. C. Baygents, R. Guzman, J. A. Schroeder, R. L. Heimark and Y. Zohar, *Lab Chip*, 2009, **9**, 1721–1731.
- 116 H. Lu, L. Y. Koo, W. M. Wang, D. A. Lauffenburger, L. G. Griffith and K. F. Jensen, *Anal. Chem.*, 2004, **76**, 5257–5264.
- 117 J. N. Lee, C. Park and G. M. Whitesides, *Anal. Chem.*, 2003, **75**, 6544–6554.
- 118 B. S. Hardy, K. Uechi, J. Zhen and H. Pirouz Kavehpour, *Lab Chip*, 2009, **9**, 935–938.
- 119 T. Gervais, J. El-Ali, A. Gunther and K. F. Jensen, *Lab Chip*, 2006, **6**, 500–507.
- 120 W. Zeng, I. Jacobi, D. J. Beck, S. Li and H. A. Stone, *Lab Chip*, 2015, **15**, 1110–1115.

- 121 J. Xu, R. Vaillant and D. Attinger, *Microfluid. Nanofluid.*, 2010, **9**, 765–772.
- 122 C. Lochovsky, S. Yasotharan and A. Gunther, *Lab Chip*, 2012, **12**, 595–601.
- 123 J. M. Karlsson, M. Gazin, S. Laakso, T. Haraldsson, S. Malhotra-Kumar, M. Maki, H. Goossens and W. van der Wijngaart, *Lab Chip*, 2013, **13**, 4366–4373.
- 124 T. Nakayama, Y. Kurosawa, S. Furui, K. Kerman, M. Kobayashi, S. R. Rao, Y. Yonezawa, K. Nakano, A. Hino, S. Yamamura, Y. Takamura and E. Tamiya, *Anal. Bioanal. Chem.*, 2006, **386**, 1327–1333.
- 125 K. Schimek, M. Busek, S. Brincker, B. Groth, S. Hoffmann, R. Lauster, G. Lindner, A. Lorenz, U. Menzel, F. Sonntag, H. Walles, U. Marx and R. Horland, *Lab Chip*, 2013, **13**, 3588–3598.
- 126 R. Lindken, M. Rossi, S. Grosse and J. Westerweel, *Lab Chip*, 2009, **9**, 2551–2567.
- 127 K. J. Jang and K. Y. Suh, *Lab Chip*, 2010, **10**, 36–42.
- 128 B. Mitchell, R. Jacobs, J. Li, S. Chien and C. Kintner, *Nature*, 2007, **447**, 97–101.
- 129 R. K. Adapala, R. J. Thoppil, K. Ghosh, H. C. Cappelli, A. C. Dudley, S. Paruchuri, V. Keshamouni, M. Klagsbrun, J. G. Meszaros, W. M. Chilian, D. E. Ingber and C. K. Thodeti, *Oncogene*, 2015, 1–9.
- 130 J. Cassuto, H. Dou, I. Czikora, A. Szabo, V. S. Patel, V. Kamath, E. Belin de Chantemele, A. Feher, M. J. Romero and Z. Bagi, *Diabetes*, 2014, **63**, 1381–1393.
- 131 S. Weinbaum, X. Zhang, Y. Han, H. Vink and S. C. Cowin, *Proc. Natl. Acad. Sci. U. S. A.*, 2003, **100**, 7988–7995.
- 132 H. J. Lee and G. Y. Koh, *Biochem. Biophys. Res. Commun.*, 2003, **304**, 399–404.
- 133 K. D. Chen, Y. S. Li, M. Kim, S. Li, S. Yuan, S. Chien and J. Y. Shyy, *J. Biol. Chem.*, 1999, **274**, 18393–18400.
- 134 Z. G. Jin, H. Ueba, T. Tanimoto, A. O. Lungu, M. D. Frame and B. C. Berk, *Circ. Res.*, 2003, **93**, 354–363.
- 135 K. Yamamoto, N. Shimizu, S. Obi, S. Kumagaya, Y. Taketani, A. Kamiya and J. Ando, *Am. J. Physiol.*, 2007, **293**, H1646–1653.
- 136 T. Ishida, T. E. Peterson, N. L. Kovach and B. C. Berk, *Circ. Res.*, 1996, **79**, 310–316.
- 137 S. Li, M. Kim, Y. L. Hu, S. Jalali, D. D. Schlaepfer, T. Hunter, S. Chien and J. Y. Shyy, *J. Biol. Chem.*, 1997, **272**, 30455–30462.
- 138 J. Chen, B. Fabry, E. L. Schiffrian and N. Wang, *Am. J. Physiol.*, 2001, **280**, C1475–1484.
- 139 N. Wang, J. P. Butler and D. E. Ingber, *Science*, 1993, **260**, 1124–1127.
- 140 M. Osawa, M. Masuda, K. Kusano and K. Fujiwara, *J. Cell Biol.*, 2002, **158**, 773–785.
- 141 U. Pohl, K. Herlan, A. Huang and E. Bassenge, *Am. J. Physiol.*, 1991, **261**, H2016–2023.
- 142 G. Siegel, M. Malmsten, D. Klussendorf, A. Walter, F. Schnalke and A. Kauschmann, *J. Auton. Nerv. Syst.*, 1996, **57**, 207–213.
- 143 J. M. Tarbell and E. E. Ebong, *Sci. Signaling*, 2008, **1**, pt8.
- 144 D. G. Harrison, J. Widder, I. Grumbach, W. Chen, M. Weber and C. Searles, *J. Intern. Med.*, 2006, **259**, 351–363.
- 145 B. P. Hierck, K. Van der Heiden, F. E. Alkemade, S. Van de Pas, J. V. Van Thienen, B. C. Groenendijk, W. H. Bax, A. Van der Laarse, M. C. Deruiter, A. J. Horrevoets and R. E. Poelmann, *Dev. Dyn.*, 2008, **237**, 725–735.
- 146 S. M. Nauli, F. J. Alenghat, Y. Luo, E. Williams, P. Vassilev, X. Li, A. E. Elia, W. Lu, E. M. Brown, S. J. Quinn, D. E. Ingber and J. Zhou, *Nat. Genet.*, 2003, **33**, 129–137.
- 147 W. A. AbouAlaiwi, M. Takahashi, B. R. Mell, T. J. Jones, S. Ratnam, R. J. Kolb and S. M. Nauli, *Circ. Res.*, 2009, **104**, 860–869.
- 148 B. C. Berk, M. A. Corson, T. E. Peterson and H. Tseng, *J. Biomech.*, 1995, **28**, 1439–1450.
- 149 S. Li, B. P. Chen, N. Azuma, Y. L. Hu, S. Z. Wu, B. E. Sumpio, J. Y. Shyy and S. Chien, *J. Clin. Invest.*, 1999, **103**, 1141–1150.
- 150 Y. M. Go, H. Park, M. C. Maland, V. M. Darley-Usmar, B. Stoyanov, R. Wetzker and H. Jo, *Am. J. Physiol.*, 1998, **275**, H1898–1904.
- 151 H. Tseng, T. E. Peterson and B. C. Berk, *Circ. Res.*, 1995, **77**, 869–878.
- 152 S. Jalali, Y. S. Li, M. Sotoudeh, S. Yuan, S. Li, S. Chien and J. Y. Shyy, *Arterioscler., Thromb., Vasc. Biol.*, 1998, **18**, 227–234.
- 153 Q. Lan, K. O. Mercurius and P. F. Davies, *Biochem. Biophys. Res. Commun.*, 1994, **201**, 950–956.
- 154 P. Carmeliet, *Nat. Med.*, 2003, **9**, 653–660.
- 155 L. Ostergaard, A. Tietze, T. Nielsen, K. R. Drasbek, K. Mouridsen, S. N. Jespersen and M. R. Horsman, *Cancer Res.*, 2013, **73**, 5618–5624.
- 156 F. le Noble, V. Fleury, A. Pries, P. Corvol, A. Eichmann and R. S. Reneman, *Cardiovasc. Res.*, 2005, **65**, 619–628.
- 157 M. Muthuchamy and D. Zawieja, *Ann. N. Y. Acad. Sci.*, 2008, **1131**, 89–99.
- 158 S. Chakraborty, M. J. Davis and M. Muthuchamy, *Semin. Cell Dev. Biol.*, 2015, **38**, 55–66.
- 159 S. Kapur, D. J. Baylink and K. H. Lau, *Bone*, 2003, **32**, 241–251.
- 160 A. Conway and D. V. Schaffer, *Stem Cell Res. Ther.*, 2012, **3**, 50.
- 161 J. Y. Shyy, *Biorheology*, 2001, **38**, 109–117.
- 162 S. S. Hur, J. C. del Alamo, J. S. Park, Y. S. Li, H. A. Nguyen, D. Teng, K. C. Wang, L. Flores, B. Alonso-Latorre, J. C. Lasheras and S. Chien, *Proc. Natl. Acad. Sci. U. S. A.*, 2012, **109**, 11110–11115.
- 163 L. Liu, K. Loutherback, D. Liao, D. Yeater, G. Lambert, A. Estevez-Torres, J. C. Sturm, R. H. Getzenberg and R. H. Austin, *Lab Chip*, 2010, **10**, 1807–1813.
- 164 E. E. Ebong, S. V. Lopez-Quintero, V. Rizzo, D. C. Spray and J. M. Tarbell, *Integr. Biol.*, 2014, **6**, 338–347.
- 165 D. Huh, B. D. Matthews, A. Mammoto, M. Montoya-Zavala, H. Y. Hsin and D. E. Ingber, *Science*, 2010, **328**, 1662–1668.
- 166 K. Hattori, Y. Munehira, H. Kobayashi, T. Satoh, S. Sugiura and T. Kanamori, *J. Biosci. Bioeng.*, 2014, **118**, 327–332.
- 167 S. Hsu, R. Thakar, D. Liepmann and S. Li, *Biochem. Biophys. Res. Commun.*, 2005, **337**, 401–409.

- 168 Y. C. Toh and J. Voldman, *FASEB J.*, 2011, **25**, 1208–1217.
- 169 I. Rizvi, U. A. Gurkan, S. Tasoglu, N. Alagic, J. P. Celli, L. B. Mensah, Z. Mai, U. Demirci and T. Hasan, *Proc. Natl. Acad. Sci. U. S. A.*, 2013, **110**, E1974–1983.
- 170 A. Hartmann, M. Stamp, R. Kmethyl, S. Buchegger, B. Stritzker, B. Saldamli, R. Burgkart, M. F. Schneider and A. Wixforth, *Lab Chip*, 2014, **14**, 542–546.
- 171 S. H. McBride, T. Falls and M. L. Knothe Tate, *Tissue Eng. Part A*, 2008, **14**, 1573–1580.
- 172 H. Chang and M. L. K. Tate, *Mol. Cell Biomech.*, 2011, **8**, 297.
- 173 R. Booth and H. Kim, *Lab Chip*, 2012, **12**, 1784–1792.